Electronic Supplementary Material (ESI) for Soft Matter.

Elastic Interactions Synchronize Beating in Cardiomyocytes - Appendices

A Method and explicit results

A.1 General Method

We define the stress-strain relationship for a linear isotropic medium by $\sigma_{ij} = \frac{E}{(1+\nu)}\left(\frac{\nu}{(1-2\nu)}\varepsilon_{kk}\delta_{ij} + \varepsilon_{ij}\right)$ and $\varepsilon_{ij} = \frac{1}{2}\left(\frac{\partial u_i}{\partial x_j} + \frac{\partial u_j}{\partial x_i}\right)$ where σ_{ij} and ε_{ij} are the stress and strain tensor respectively, and $x_i, x_j \in (x, y, z)$ are the principal axes in Cartesian space, while E,ν are the Young's modulus and Poisson ratio respectively. Using these definitions in Eq. 1 yields Eq. 2 that appears in the text. This can further be written in matrix form as:

$$\mathcal{M}\vec{u} = -\vec{f} \ , \quad \mathcal{M}_{ij} = \alpha_{kk}\delta_{ij} + \beta_{ij}(1 - \delta_{ij}) \tag{A.1}$$

Here $\mathcal{M}$ is a 3X3 response matrix with $\alpha(\beta)$ the diagonal(off-diagonal) elements which are determined by the expressions for the viscous forces f_v listed in Table 1.

The force exerted by the cell (or probe) is modeled by two equal and opposite contractile forces. separated by a distance z_0 along the z-axis. Thus $f_x = f_y = 0$ and the contraction along the z-axis is given by:

$$f_z = -F(\delta(z - z_0) - \delta(z + z_0))G(t) \tag{A.2}$$

where $G(t) = \Theta(t)$ is the Heaviside theta function (step function) for the static contraction, and $G(t) = 1/2(1 + \cos(\omega_0 t))\Theta(t)$ for the dynamically oscillating force. To further simplify the calculations we use the dipole approximation limit in which the distance between the probe and cell (or the two cells) is much greater than the cell size ($r \gg z0$).

We define the Fourier transform $f(\vec{q})$ of any function in real space $f(\vec{r})$ as

$$f(\vec{q}) = \frac{1}{\sqrt{2\pi}}\int_{-\infty}^{\infty} f(\vec{r})e^{i\vec{q}\cdot\vec{r}}d\vec{r} \tag{A.3}$$

and the inverse Fourier transform as

$$f(\vec{r}) = \frac{1}{\sqrt{2\pi}}\int_{-\infty}^{\infty} f(\vec{q})e^{-i\vec{q}\cdot\vec{r}}d\vec{q} \tag{A.4}$$

where $\vec{q}$ is defined in spherical coordinates with boundaries $0 < q < \infty$, $0 < \theta < \pi$, $0 < \phi < 2\pi$. The temporal Fourier transform is defined as:

$$f(\vec{\omega}) = \frac{1}{\sqrt{2\pi}}\int_{-\infty}^{\infty} f(t)e^{it\omega}dt \tag{A.5}$$

The q-space expression for the temporal Fourier transform of the displacement thus becomes:

$$\begin{aligned}
u_x(q,\omega) &= \frac{2Fz_0(1+\nu)}{E(1-\nu)}\frac{q^3\sin\theta\cos^2\theta\cos\phi G(\omega)}{\left(q^2 - \frac{2i\gamma(1+\nu)\omega}{E}\right)\left(q^2 - \frac{i\gamma(1+\nu)(1-2\nu)\omega}{E(1-\nu)}\right)} \\
u_y(q,\omega) &= \frac{2Fz_0(1+\nu)}{E(1-\nu)}\frac{q^3\sin\theta\cos^2\theta\sin\phi G(\omega)}{\left(q^2 - \frac{2i\gamma(1+\nu)\omega}{E}\right)\left(q^2 - \frac{i\gamma(1+\nu)(1-2\nu)\omega}{E(1-\nu)}\right)} \\
u_z(q,\omega) &= -\frac{2Fz_0(1+\nu)}{E(1-\nu)}\frac{q\cos\theta\left(q^2\left(\sin^2\theta + \frac{(1-2\nu)}{2(1-\nu)}\right) - \frac{i\gamma\omega(1+\nu)(1-2\nu)}{E}\right)G(\omega)}{\left(q^2 - \frac{2i\gamma(1+\nu)\omega}{E}\right)\left(q^2 - \frac{i\gamma(1+\nu)(1-2\nu)\omega}{E(1-\nu)}\right)}
\end{aligned} \tag{A.6}$$

with $G(\omega)$ the Fourier transform of the expression for a static, or dynamic dipole as described above. We then use the definition of the inverse transform to obtain the real space displacement $u_i(\vec{r})$. To obtain the strain ε_{ij}, we differentiate the expression for u_i in q-space, which correspond to multiplication by a factor of $-iq_i$, and apply the inverse transform.

A.2 Static dipole solution

For simplicity, we examine the propagation of the elastic signal along the three principal directions. Note that due to rotational symmetry of the geometry, the x and y components of the displacement field u_i are identical. The same goes for the respective components of the strain field ε_{ij} where i or j are either x or y.

The displacement field (along the x, and z axes) induced by a static force dipole of magnitude $P = Fz_0$ that begins to contracts at time $t = 0$ (and remains contracted for $t > 0$) is given by:

$$\begin{aligned} u_x(r,0,0,t) = \; & \tfrac{Fz_0(1+\nu)}{8\pi E(1-\nu)r^2}\Big[1+\tfrac{1}{(\chi_s^2-\chi_c^2)}\Big\{\tfrac{3}{\sqrt{\pi}}\left(\chi_c e^{-\chi_c^2}-\chi_s e^{-\chi_s^2}\right) \\ & +\left(\chi_c^2-\tfrac{3}{2}\right)\mathrm{erf}(\chi_c)-\left(\chi_s^2-\tfrac{3}{2}\right)\mathrm{erf}(\chi_s)\Big\}\Big] \\ u_z(0,0,r,t) = \; & -\tfrac{Fz_0(1+\nu)}{4\pi E r^2}\Big[1+\tfrac{1}{\chi_s^2}\Big\{\tfrac{3}{\sqrt{\pi}}\left(\chi_c e^{-\chi_c^2}-\left(\chi_s+\tfrac{2}{3}\chi_s^3\right)e^{-\chi_s^2}\right) \\ & +\left(\chi_c^2-\tfrac{3}{2}\right)\mathrm{erf}(\chi_c)+\tfrac{3}{2}\mathrm{erf}(\chi_s)\Big\}\Big] \end{aligned} \tag{A.7}$$

We defined two new dimensionless variables, $\chi_c = \sqrt{\frac{\gamma(1+\nu)(1-2\nu)r^2}{4E(1-\nu)t}}$ and $\chi_s = \sqrt{\frac{\gamma(1+\nu)r^2}{2Et}}$ (where for u_x, $r = x$ and for u_z, $r = z$), corresponding to the two modes of signal propagation in our system (compressional mode and shear mode respectively). The elastic signal propagates into the medium from the dipole in a diffusion-like manner. At time $t = 0$ the deformation begins to propagate into the matrix from the dipole until,at long times ($\chi_i \gg 1$), the deformation relaxes to its equilibrium value, noted by $u_i^{eq}(x,y,z)$:

$$\begin{aligned} u_x^{eq}(r,0,0) = \; & \tfrac{Fz_0(1+\nu)}{8\pi E(1-\nu)r^2} \\ u_z^{eq}(0,0,r) = \; & -\tfrac{Fz_0(1+\nu)}{2\pi E r^2} \end{aligned} \tag{A.8}$$

Additionally, one can calculate the equilibrium strain in the medium along the axes $\varepsilon_{ij}^{eq}(x,y,z)$ by taking the spatial derivative of the displacement:

$$\begin{aligned} \varepsilon_{xx}^{eq}(r,0,0) = \; & -\tfrac{Fz_0(1+\nu)}{4\pi E(1-\nu)r^3} \\ \varepsilon_{zz}^{eq}(r,0,0) = \; & \tfrac{Fz_0(1+\nu)(4\nu-1)}{4\pi E(1-\nu)r^3} \\ \varepsilon_{zz}^{eq}(0,0,r) = \; & \tfrac{Fz_0(1+\nu)}{\pi E r^3} \end{aligned} \tag{A.9}$$

Note that the steady-state displacement has a power law decay proportional to r^{-2} (r^{-3} for the strain).

The characteristic time scale for relaxation depends on the distance between the point of interest in the medium and the dipole as well as the viscosity of the medium through which the strain and stress propagate. In the limit of an incompressible matrix ($\nu \to 1/2$) the compressional mode propagates infinitely fast. In this case, the system is dominated by the shear mode. Thus, we focus on the shear mode denoted by the dimensionless variable χ_s. The friction coefficient γ can be estimated using the properties of the matrix from $\gamma = \eta/d^2$ where η is the kinematic viscosity of water and d is the characteristic pore size within the polymeric network of the gel [1]. For cells in hydrogel matrices, we estimate $d \approx 15$ nm [2] which yields $\gamma \approx 3.5 * 10^{12}$ Pa·s/m^2 . By taking the gel to be nearly incompressible ($\nu = 0.49$) and with a stiffness $E = 10$ kPa (comparable to biological tissue), we calculate the time required for the elastic signal to travel a distance of $r = 100$ μ m of the order of 1 second.

A.3 Oscillating dipole solution

We list here the full expressions of the displacement and strain fields presented in the text. The steady state displacement $u_i^{ss}(x,y,z,t)$, and strain $\varepsilon_{ij}^{ss}(x,y,z,t)$, due to a dynamically oscillating force dipole, can be written as a sum of a static part denoted by the superscript "eq" (defined by Eq. A.8,A.9), and an additional dynamical part written in capital letters:

$$\begin{aligned} u_i^{ss}(x,y,z,t) &= \tfrac{1}{2}[u_i^{eq}(x,y,z) + U_i(x,y,z,t)] \\ \varepsilon_{ij}^{ss}(x,y,z,t) &= \tfrac{1}{2}[\varepsilon_{ij}^{eq}(x,y,z) + E_{ij}(x,y,z,t)] \end{aligned} \tag{A.10}$$

The explicit result for the displacement along each axis is given by:

$$\begin{aligned} u_x^{ss}(r,0,0,t) = \frac{Fz_0(1+\nu)}{16\pi E(1-\nu)r^2}\Big[1 + \frac{1}{\rho_s^2-\rho_c^2}\big[e^{-\rho_c}\left((3\rho_c+2\rho_c^2)\cos\Omega_c) + (3+3\rho_c)\sin(\Omega_c)\right) \\ -e^{-\rho_s}\left((3\rho_s+2\rho_s^2)\cos(\Omega_s) + (3+3\rho_s)\sin(\Omega_s)\right)\big]\Big] \\ u_z^{ss}(0,0,r,t) = -\frac{Fz_0(1+\nu)}{4\pi E r^2}\Big[1 + \frac{1}{\rho_s^2}\big[e^{-\rho_c}\left((3\rho_c+3\rho_c^2+\rho_c^3)\cos(\Omega_c) + (3+3\rho_c-\rho_c^3)\sin(\Omega_c)\right) \\ -e^{-\rho_s}\left((3\rho_s+2\rho_s^2)\cos(\Omega_s) + (3+3\rho_s)\sin(\Omega_s)\right)\big]\Big] \end{aligned} \tag{A.11}$$

and the steady state strain along the axes is:

$$\varepsilon_{zz}^{ss}(0,0,r,t) = \frac{Fz_0(1+\nu)}{2\pi E r^3}\Big[1+\frac{1}{\rho_s^2}\Big(e^{-\rho_c}\Big((6\rho_c+6\rho_c^2+2\rho_c^3)\cos(\Omega_c)+(6+6\rho_c+2\rho_c^3-\rho_c^4)\sin(\Omega_c)\Big) \\ -e^{-\rho_s}\Big((6\rho_s+5\rho_s^2+\rho_s^3)\cos(\Omega_s)+(6+6\rho_s-\rho_s^3)\sin(\Omega_s)\Big)\Big)\Big]$$

$$\varepsilon_{zz}^{ss}(r,0,0,t) = \frac{Fz_0(1+\nu)(4\nu-1)}{8\pi E(1-\nu)r^3}\Big[1+\frac{1}{\rho_s^2-3\rho_c^2}\Big(e^{-\rho_c}\left((9\rho_c+8\rho_c^2+2\rho_c^3)\cos(\Omega_c)+(9+9\rho_c-\rho_c^3)\sin(\Omega_c)\right) \\ -e^{-\rho_s}\left((9\rho_s+6\rho_s^2)\cos(\Omega_s)+(9+9\rho_s-3\rho_s^3)\sin(\Omega_s)\right)\Big)\Big]$$

$$\varepsilon_{xx}^{ss}(0,0,r,t) = \varepsilon_{xx}^{ss}(r,0,0,t) = -\frac{Fz_0(1+\nu)}{4\pi E(1-\nu)r^3}\Big[1+\frac{1}{\rho_s^2-\rho_c^2}\Big(e^{-\rho_c}\big(\big(6\rho_c+5\rho_c^2+\rho_c^3\big)\cos(\Omega_c) \\ +\big(6+6\rho_c-\rho_c^3\big)\sin(\Omega_c)\big)-e^{-\rho_s}\big(\big(6\rho_s+5\rho_s^2+\rho_s^3\big)\cos(\Omega_s)+\big(6+6\rho_s-\rho_s^3\big)\sin(\Omega_s)\big)\Big)\Big] \tag{A.12}$$

Here we define the dimensionless parameters $\rho_c = \kappa_c r$, $\rho_s = \kappa_s r$ (based on the notations in the text), and $\Omega_i = \omega_0 t - \rho_i$

Note that the time dependent terms in both the displacement and strain decay exponentially in space as $\exp[-\kappa_i r]$, and that this exponential decay is not the same as the diffusive response of the transient term as discussed above for the static case. To better understand that, we calculate the root mean square of the dynamical part of the displacement $U_i^{dy}(x,y,z,t)$ (and strain $E_{ij}(x,y,z,t)$), using Eq. 6 averaged over a time of one cycle, $T = 2\pi/\omega_0$:

$$RMS(r,\kappa_c,\kappa_s) = \sqrt{< U_i^2 >} = \left(\frac{\omega_0}{2\pi}\int_0^{\frac{2\pi}{\omega_0}} U_i^2 \; dt\right)^{1/2} \tag{A.13}$$

with a similar formula used for the strain. In Fig. A.1 we plot, as an example, the RMS of the displacement and strain as a function of the distance between the probe and cell r, for both incompressible ($\nu = 0.5$) and completely compressible ($\nu = 0$) media, using the parameters $E = 10^4$ Pa, $\gamma = 3.5 \cdot 10^12$ Pa·s/m^2 and $\omega_0 = 2\pi$ rad/s. Note that in all cases, the dynamical contribution decays as a power law up to $r \approx 100\mu$m, but than begins to decay exponentially (much faster in space). This is a demonstration of the role of the dynamical length scale $1/\kappa_c$ discussed in the text.

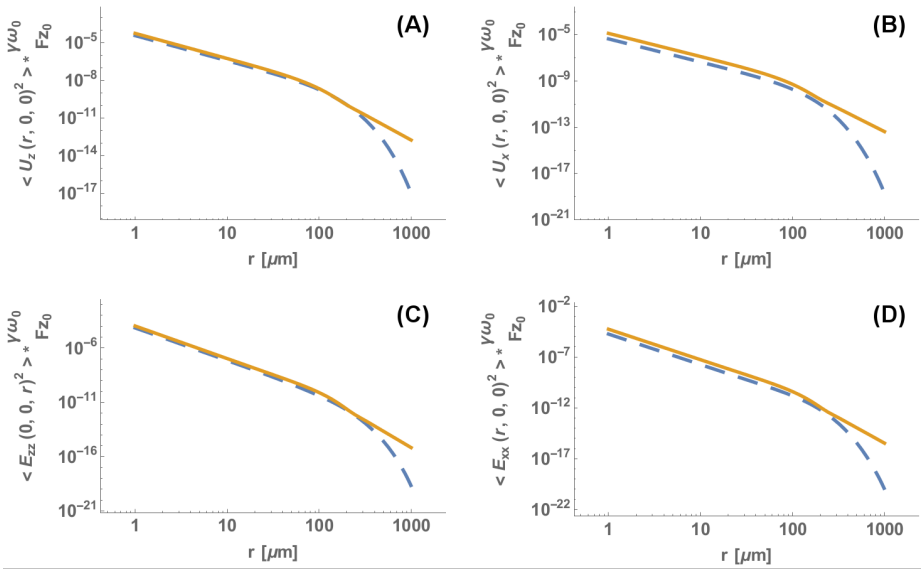

Figure A.1: RMS of the dynamical contribution of the displacement (A,B) and strain (C,D), normalized by $Fz_0/\gamma\omega_0$, as a function of distance r away from the dipole The results of Eq. A.13 (and the similar equation for the strain) are plotted on a log-log scale, and the chosen parameters are $E = 10^4$ Pa, $\gamma = 10^{12}$ Pa·s/m^2 and $\omega_0 = 2\pi/T$ where $T = 1$ sec. The full–orange line corresponds to a Poisson ratio $\nu = 0.5$, and the dashed–blue line corresponds to a Poisson ratio $\nu = 0$.

B Matrix deformation as a function of phase of two, non-interacting, beating force dipoles.

Since the medium is linearly elastic, all deformations induced by external forces (dipoles) are additive. This is evident by examining the case of two, non-interacting nearby dipoles as in Fig. B.1, both aligned along the z-axis, and a distance x_0 apart along the x-axis (one located at $x = -x_0/2$ and the other at $x = x_0/2$).

Note that for this new geometry, the x and y axes are no longer equivalent by symmetry. In this case dipoles beat at the same frequency, and can have a phase difference ψ that is constant and which, in general, might be different from zero since their beating is not necessarily activated at the same time. This is applicable to two sarcomeric units beating in close proximity or, on a larger scale, two nearby cardiomyocytes.

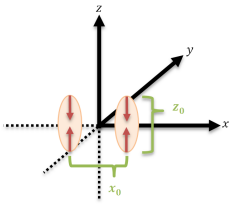

Figure B.1: A pair of force dipoles that are oriented along the z-axis and separated by a distance x_0 along the x-axis.

We calculate the time dependent displacement of the medium under steady-state conditions (using superposition, as appropriate to a linear elastic medium). One can show that in this case, the oscillatory, steady-state displacement in the matrix $u_i^{os,2}$ due to the superposition of the two dipoles perpendicular to the line joining the two dipoles (i.e., along the z and y axes) is:

$$\begin{aligned} u_y^{os,2}(0,r,0,t) &= 2u_y^{os}\cos\frac{\psi}{2} \\ u_z^{os,2}(0,0,r,t) &= 2u_z^{os}\cos\frac{\psi}{2} \end{aligned} \tag{B.1}$$

If both dipoles beat in-phase ($\psi = 0$) the displacement of the medium between the cells is effectively doubled while if the two beat in anti-phase ($\psi = \pi$) they cancel each other's effect and the displacement of the medium is zero. This simple result is an outcome of the dipole approximation ($z_0 \ll r$). In the immediate vicinity of both cells there can be additional effects due to the finite spacing between the two force centers that comprise the dipole; in the dipole approximation this distance is taken to be much smaller than the distance at which the strain or stress are considered.
For the deformations of the medium along x-axis, we take the limit of $x_0 << r$ and expand the superimposed solution for two dipoles separated by a distance

x_0 along the x direction to find:

$$u_x^{os,2}(r,0,0,t) = 2\left(u_x^{os}\cos\frac{\psi}{2} + \frac{x_0}{r}U^{os}(\rho_c,\rho_s)\sin\frac{\psi}{2}\right) \tag{B.2}$$

Where U^{os} is a time independent function of ρ_c, ρ_s, similar to u_x^{os}, which tend to 0 for $\rho_i \to \infty$ and to a decay that scales as r^{-2} for $\rho_i \to 0$. This implies that both in-phase and out-of-phase terms decay in the same manner for regions in the medium that are far from both dipoles, but at small distances, the finite separation between cells allows the possibility of an out-of-phase component. It can thus be seen that between the two dipoles (and as long as $\kappa_c x_0 < 1$), an out-of-phase term is present due to the finite velocity of signal propagation in the dissipative medium. By taking the limit of close proximity ($x_0 \to 0$), a quadrupole is essentially created and the out-of-phase term vanishes.

C Derivation of the elastic free energy

In this appendix, we show how the elastic deformation energy of the matrix that reflects the interaction due to the work performed by one contractile cell against the displacement of the matrix induced by the nearby cell or probe, can be written in the form of Eq. 4, as the product of the force dipole of one cell with the strain induced by the other cell. This energy gives rise to a stress (given by the derivative of the energy with respect to the strain [3]) whose divergence in space (as a function of the distance between the two cells) results in a force that acts on the adhesions of the cell (see Eq. 5). We note that the total elastic deformation energy of the matrix also includes terms (usually called "self energies") in which the forces of a given cell interact with the displacements caused by the same cell. But these are not relevant to the forces exerted by one cell upon the other and we thus focus only on the "interaction" terms and not on the "self energies".

We begin with the Green's function for a point force located at $\vec{r'}$ in an infinite elastic medium, which is a function of the distance from said point $|\vec{r} - \vec{r'}|$, and is given by [3]:

$$G_{ij}(\vec{r} - \vec{r'}) = \frac{(1+\nu)}{2\pi E}\left[\frac{\delta_{ij}}{|\vec{r} - \vec{r'}|} - \frac{1}{4(1-\nu)}\frac{\partial(|\vec{r} - \vec{r'}|)}{\partial x_i \partial x_j}\right] \tag{C.1}$$

where x_i, x_j are any of the principal directions in Cartesian space (x, y, z), ν is the Poisson ratio and E the Young's modulus. The deformation induced by a point-force F_i located at $\vec{r'}$ is given by $u_j(\vec{r}) = F_i G_{ij}(\vec{r} - \vec{r'})$. The deformation energy, H, that arises from the work done by a local force located at $\vec{r}$ (say, one end of the cell) interacting with the displacement of the medium generated by a second point force at $\vec{r'}$ (say, a probe or one end of another cell) is a scalar quantity, and is thus given by:

$$H = F_j u_j(\vec{r}) = F_j F_i \; G_{ij}(\vec{r} - \vec{r'}) \tag{C.2}$$

where we use the summation convention over repeated indices. Note that since this is a scalar product, the components of the force vector in each direction are coupled only to the components of the displacement along the same direction. For example, a point force located at $\vec{r} = 0$ that acts in the z-direction ($F_x = F_y = 0$, $F_z \neq 0$) is coupled only to the local deformation at $\vec{r} = 0$ induced by the second point force located at $\vec{r'}$, along the same direction (i.e, $u_z(0)$). Thus, we can always choose the coordinate system so that one force points along any of the major axes, and interacts with the displacement induced by another force (pointing in a general direction) along that same axis, without loss of generality.

We now examine the special case of a cell comprising two equal and opposite forces separated by a vector distance $\vec{a}$, with the center between the two forces located at point $\vec{r'}$. This description is appropriate in the case of needle-like cells as discussed in the main text. The displacement induced by such a cell at

any point $\vec{r}$ is written as:

$$u_j^d(\vec{r}) = F_i \; G_{ij}^d(\vec{r} - \vec{r'}, \vec{a}) = F_i \left[G_{ij}(\vec{r} - (\vec{r'} - \vec{a}/2)) - G_{ij}(\vec{r} - (\vec{r'} + \vec{a}/2)) \right] \tag{C.3}$$

For $\vec{r} - \vec{r'} \gg \vec{a}$, we expand the Green's function in powers of the inter force distance a:

$$G_{ij}^d(\vec{r} - \vec{r'}, \vec{a}) \approx a_k \left. \frac{dG_{ij}^d}{da_k} \right|_{\vec{a}=0} = a_k \; \frac{dG_{ij}}{dr'_k}(\vec{r} - \vec{r'}) \tag{C.4}$$

where the displacement field arising from this approximation can be written in terms of the force dipole moment $p_{ij} = F_i a_j$ and the derivative of the Green's function $G_{ij,k'}(\vec{r} - \vec{r'}) = \frac{dG_{ij}}{dr'_k}(\vec{r} - \vec{r'})$:

$$u_i^d(\vec{r}) = p_{jk} G_{ij,k'}(\vec{r} - \vec{r'}) \tag{C.5}$$

We now examine the interaction energy of such a "dipole" as a representation of a cell located at $\vec{r'}$, with another needle-like cell with the center located at $\vec{r}$, comprising two equal and opposite point forces separated by a vector distance $\vec{a}$. The interaction energy in this case can be written as:

$$H = F_i u_i^d(\vec{r}) = F_i \; p_{jk} \left[G_{ij,k'}((\vec{r} + \vec{a}/2) - \vec{r'}) - G_{ij,k'}((\vec{r} - \vec{a}/2) - \vec{r'}) \right] \tag{C.6}$$

Again, by taking the same limit as above (small $\vec{a}$), the sum of the two forces at both ends of the cell cancels, and one must expand the Green's function $G_{ij,k'}$ to get:

$$H = F_i \; a_l \; p_{jk} \; \frac{dG_{ij,k'}}{dr_l}(\vec{r} - \vec{r'}) = p_{il} \; p_{jk} G_{ij,k'l}(\vec{r} - \vec{r'}) \tag{C.7}$$

We therefore see that for the case of two needle-like cells of length $|\vec{a}|$, separated by a distance $\vec{r} - \vec{r'} \gg \vec{a}$, the only contribution to the elastic energy is from the second derivative of the Green's function. If we now define the local strain at $\vec{r}$, induced by a cell located at $\vec{r'}$ as $\varepsilon_{ik}(\vec{r}) = p_{jk} G_{ij,k'l}(\vec{r} - \vec{r'})$ we can write the total interaction energy of the two cells (using symmetry) as:

$$H = 2 p_{ij} \; \varepsilon_{ij}(\vec{r}) \tag{C.8}$$

This is equivalent to the interaction energy of Eq. 4 in the main text. This derivation demonstrates that in the dipole approximation, the only contribution to the elastic energy of the medium comes from the local strain (and not the local displacement) induced at point $\vec{r}$ by a cell located at $\vec{r'}$.

D Near-field solution (where dipole approximation fails)

The dipole approximation is generally valid for distances $r \gg z_0$, and is thus a far-field description. The spatial dependence of the near-field displacement or strain may be relevant experimentally, since the probe that paces the cell may not be much further from the cell than the typical cell size, z_0. We therefore derive the displacement field for two point forces, in the case of both static and oscillating forces, and compare the results to the dipole approximation. Here we must make a more refined assumption for the spatial position along each axis, since the displacement field behaves quite differently along the z-axis and the x,y-axes.

We first consider the static case. For u_z, the displacement field has two distinct regimes, inside ($-z_0/2 < z < z_0/2$) and outside ($z < -z_0/2, z > z_0/2$) of the dipole. Since we are more interested in interactions between isolated cells, we concentrate on the latter regime. In the outer regime, the displacement field along the z-axis (aligned with the dipole) is:

$$\begin{aligned} u_x^{ss}(r,0,0) = &\quad \tfrac{F(1+\nu)z_0 r}{4\pi E(1-\nu)(r^2-(z_0/2)^2)^{3/2})} \qquad r>0 \\ u_z^{ss}(0,0,r) = &\quad -\tfrac{F\pi z_0(1+\nu)}{2\pi E(r^2-(z_0/2)^2} \qquad r>z_0/2 \end{aligned} \tag{D.1}$$

Note that by taking the limit of $z_0 \to 0$ and $F \to \infty$ (so that their product – which is the force dipole moment – remains constant) we recover the static solution of Eq. A.8. To evaluate at what distance both solutions coincide we examine the ratio R_i of the dipole solution (Eq. A.8) and the monopoles solution (Eq. D.1)

$$R_x = \tfrac{r^2-(z_0/2)^2}{r^2} = (1-\tfrac{1}{4}\left(\tfrac{z_0}{r}\right)^2)^{3/2}$$

$$R_z = \tfrac{r^2-(z_0/2)^2}{r^2} = 1-\tfrac{1}{4}\left(\tfrac{z_0}{r}\right)^2$$

The dipole approximation is thus suitable for $z_0 \ll r$. Along the x-axis, the dipole approximation is valid within 10% error ($R_x = 0.9$) at a distance of roughly the cell size away from the poles ($r \approx 2z_0$), while for the z-axis, the dipole approximation is valid within 10% for a distance of roughly half a cell size ($r \approx 1.5z_0$).
For the case of an oscillating force, we again focus on the region outside of the dipole (by assuming $z > z_0/2$), and solve, as an example, for the oscillatory displacement field on the z-axis:

$$\begin{aligned} u_z^{os}(0,0,r,t) = \frac{Fz_0}{2\pi\omega_0\gamma}\sum_{n=1,2}\Bigg[&\frac{e^{-\rho_{c,n}}}{\zeta_n^3}\left(\rho_{c,n}\cos\left(\omega_0 t-\rho_{c,n}\right)+(1+\rho_{c,n})\sin\left(\omega_0 t-\rho_{c,n}\right)\right) \\ &-\frac{e^{-\rho_{s,n}}}{\nu_n^3}\left((\rho_{s,n}-\rho_{s,n}^2)\cos\left(\omega_0 t-\rho_{s,n}\right)+(1+\rho_{s,n})\sin\left(\omega_0 t-\rho_{s,n}\right)\right)\Bigg] \end{aligned} \tag{D.2}$$

where we defined for convenience $\zeta_1 = (r-z_0/2)$, $\zeta_2 = (r+z_0/2)$ and $\rho_{c,n} = \kappa_c\zeta_n$ and $\rho_{s,n} = \kappa_s\zeta_n$ with κ_c,κ_s as defined in the text.

Note that the expression contains minor corrections to the previously used distance from the cell r , since we now take into account the spatial distribution of poles. However, taking the limit of $z \gg z_0$ and expanding in a Taylor series up to linear order, reduces to the strain as given by the dipole approximation, as expected. Although we cannot use the same analysis as above to estimate the point of 10% error, due to the exponential nature of both functions, we may guess the solutions coincide for z/z_0 of order unity (a single cell length as above). These results show that the qualitative behavior for a force dipole remain the same, even when the distance between the probe and the cell (or between two cells) is comparable with the size of the cell itself.

We consider two generic situations that are relevant for a cell that is in a matrix deformed by another cell or probe. The first case we consider is when the cell is relatively close (a distance of the order of the cellular size z_0) to the source of the local deformations (another cell or a probe). In this case, the cell cannot be accurately described by a force dipole, and one must consider the more accurate picture of two equal and opposite point forces separated by a distance z_0. As we show in Appendix C, the interaction energy in this case is given by the scalar product of the force applied by the cell at $\vec{r}$ with the local displacement field $\vec{u}(\vec{r})$ due to the other cell (or probe). Note that the forces are coupled only to the components of the displacement that are in the same direction. Thus, force vectors pointing along the z-direction are coupled only to the z-component of the deformation field caused by a nearby cell or probe (see Appendix C).

In the top row of Fig. D.1 we plot (A) the static displacement of the medium $u_z(\vec{r})$ induced by a force dipole p_{zz} located at the origin, (B) the superimposed displacement fields of two equal and oppositely directed point forces that act in the z-direction and are located at $x = y = 0,\ z = \pm z_0/2$ and (C) a force monopole that acts along the x direction and is located at the origin. The first two panels (A and B) represent the displacement in the medium induced by a neighboring cell, while the third panel (C) represent the displacement in the medium due to a probe as in Tzlil's experiments. Note that in all cases,for a symmetric, needle-like cell oriented along the z-direction (whose center is located at $z = 0$ and a distance x from the origin, $x \gg z_0$), the displacement field is antisymmetric as a function of z so that the cellular force at $(x, z_0/2)$ (pointing in the $-z$ direction) acts on a region of the matrix whose displacement is positive, while the force at $(x, -z_0/2)$ (pointing in the $+z$ direction) acts on a region of the matrix whose displacement is negative. Thus, for a contractile cell, contraction always occur in a direction opposite to the displacement in the medium, which lowers the its elastic energy. Conversely, when the cell is close to the source of deformations ($x \leq z_0$), the spatial separation of the forces within the cell can become important, because as the separation of forces z_0 increases there is a crossover to a regime where the force located at $(x, z_0/2)$ acts on a matrix displaced in the negative direction, and the force at $(x, -z_0/2)$ acts on a matrix displaced in the positive direction. In that case, contraction always increase the total elastic energy of the medium.

Extending these ideas to time dependent, oscillatory deformations, this implies that if cells are close enough, this could potentially cause an "anti-phase"

beating behavior. "Anti-phase" beating can also be induced by changing the elasticity of the medium, as presented in Fig. 3B in and discussed in the text. Finally, for the situation in which the cell at $\vec{r}$ is modeled by two point forces that are close to the source of the deformations, the assumption that changes in cell length z_0, resulting from the mechanical deformations of the matrix, are negligible might also be incorrect. The additional time dependent size $z_0(t)$ adds another layer of complexity that might also promote "in-phase" synchronization. All of these effects require a more detailed model which is beyond the scope of our treatment whose goal is to examine the simplest, generic situation.

The second general case that one can think of is when the cell is far enough from the source that the effects of its size are negligible. This is the case discussed in the text, where the cell is modeled as a force dipole, and the major contribution to the interaction energy is from the product of the force dipole and the external strain (see Eq. 4 in the text and explanation in Ap. C).

In the bottom row of Fig. D.1 we compare (D) the strain field $\varepsilon_{zz}(r)$ induced by a force dipole p_{zz} located at the origin, (E) two equal and opposite forces acting on the z-direction and located at $x = y = 0,\ z = \pm z_0/2$, and (F) a force monopole located at the origin and aligned along the x-axis. One can see that the variation of the zz component of the strain as a function of the distance of the cell from the probe along the x-axis, is similar in all three cases. This implies that the results of "in-phase" beating should be similar, regardless of the way one models the probe.

Finally, Tzlil [4] has reported that when the probe is oscillated in the z-direction, the cells do not synchronize with the phase and frequency of the probe. In this case, for a probe modeled as a force monopole aligned along z-direction and located at the origin, both ends of a cell which are located at $z = \pm z_0/2$ and a distance x from the probe are subjected to the same magnitude and sign of deformation/strain along the z-direction. This means (since the forces are equal and opposite while the displacements at $+z_0$ and $-z_0$ are the same) that the cellular force acting on the matrix displacement causes an increase in matrix elastic energy at one end and a decrease at the other so that both effects cancel by symmetry. Therefore, contraction of the cell in phase or in synchrony with the probe does not contribute to the medium elastic energy when the probe deforms the matrix in the z direction. This argument can be extended to the dynamical steady-state interactions through averaging, as described in the text. Again, the temporal average of deformations near the cell is zero due to symmetry, so no modification of phase and frequency is observed. If, however, the experiments were to be performed with a probe that "pinches" the substrate (and is therefore better described by a dynamic force dipole), we predict that the cell will synchronize in a manner that is dictated by the mutual orientation of cell and probe, as described in the text.

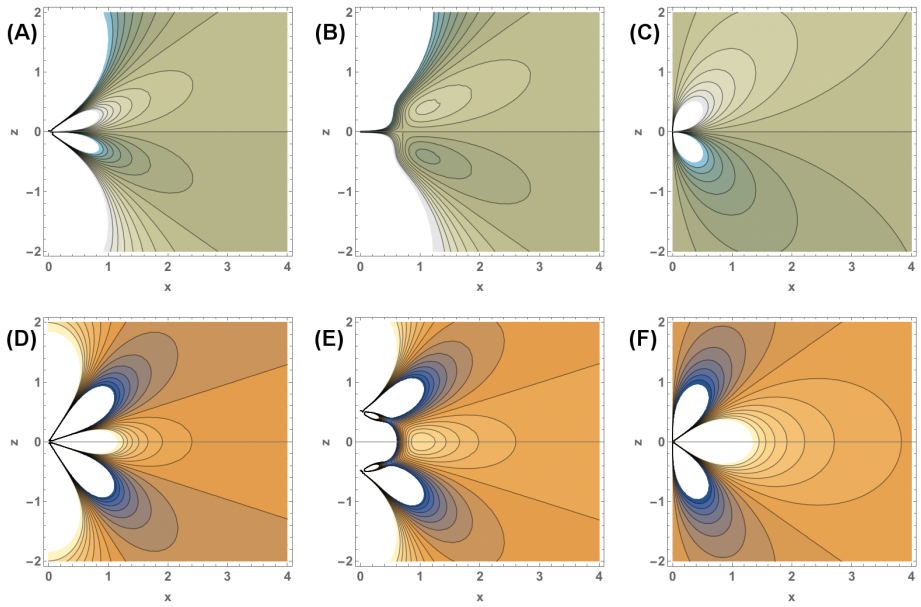

Figure D.1: Displacement u_z (top) and strain component ε_{zz} (bottom) in an incompressible medium ($\nu = 0.5$) for (A,D) a force dipole located at the origin and aligned along the z-axis, (B,E) two equal and opposite point forces aligned along the z-axis, a distance $z_0 = 1$ apart and (C,F) a point force aligned along the x-axis. Both x and z axes are measured in units of z_0. Lighter shades (green,yellow) correspond to positive values, while darker shades (blue) to negative values.

E Other Forms of Friction

We address here two additional models for visco-elastic friction, as presented in Table 1 in the text. For each model, we present the displacement field induced by either static contraction or dynamical beating with fixed frequency. We then briefly discuss the interactions of two oscillating dipoles and how those differ from the "simple friction" model. We apply the same methods as described in appendix A and discuss details only as necessary.

E.1 Local dissipation model (Kelvin-Voigt)

The local dissipation model, also known as the Kelvin-Voigt model describe a frictional force with no spatial dependence (see Table 1). One can relate the dissipation of energy in this model to the friction that arises form the motion of the polmyers comprising the gel that move against each other. One of the key features of this model is that it assumes that dissipation is uniform everywhere inside the medium. An analogous 1-D system for this model is a spring and dashpot connected in parallel. By pulling on such a construct, some of the energy gets stored in the spring, while some get dissipated through the dashpot. Terms in Eq. 2 that involve the gradient now involve an additional term proportional to $d\vec{u}/dt$. This spatially uniform dissipation of energy gives rise to an infinitely fast propagation of elastic signals. Note that the Kelvin-Voigt model predicts solid like elastic response at long time scales, and not fluid-like, viscous flow, making it relevant for our case of cells adhered to a hydro-gel substrate. In this model, the shear and bulk viscosities are given by η_1, η_2 respectively. Using the expression for $\vec{f_v}$ in Table 1, the displacement field for static contraction becomes:

$$\begin{aligned} u_x(r,0,0,t) &= \tfrac{Fz_0(1+\nu)}{4\pi E(1-\nu)r^2}\left(1+\tfrac{(1-2\nu)}{2}e^{-t/\tau_s}-(1-\nu)e^{-t\tau_c}\right) \\ u_z(0,0,r,t) &= -\tfrac{Fz_0(1+\nu)}{4\pi Er^2}(1-e^{-t/\tau_s}) \end{aligned} \tag{E.1}$$

Here we define the characteristic time scales $\tau_s = \frac{2\eta_2(1+\nu)}{E}$ and $\tau_c = \frac{(\eta_1+2\eta_2)(1+\nu)(1-2\nu)}{E(1-\nu)}$ corresponding to the shear and compressional modes.

It can be seen immediately that aside from the normal r^{-2} decay the displacement has no spatial dependence since the viscoelastic response is spatially uniform and is characterised by an exponential decay in time. Once the dipole is "turned on" at time $t = 0$ and statically contracts, the viscous response dictates the time required for the medium to stabilize, but the elastic response is carried instantly throughout.

For the oscillating force dipole, the steady-state displacement of the oscillatory part is given by:

$$\begin{aligned} u_x^{os}(r,0,0,t) &= \tfrac{Fz_0(1+\nu)}{4\pi E(1-\nu)r^2}\sqrt{\tfrac{(1+(\omega_0\tau_a)^2)}{(1+(\omega_0\tau_c)^2)(1+(\omega_0\tau_s)^2)}}\cos(\omega_0 t-\Phi_x) \\ u_z^{os}(0,0,r,t) &= -\tfrac{Fz_0(1+\nu)}{4\pi Er^2}\sqrt{\tfrac{1}{1+(\omega_0\tau_s)^2}}\cos\left(\omega_0 t-\Phi_z\right) \end{aligned} \tag{E.2}$$

where we define another time scale $\tau_a = \frac{2(\eta_1+\eta_2)(1+\nu)(1-2\nu)}{E}$. Here, the phase difference Φ_i is spatially independent, dictated only by the viscous response of the medium:

$$\Phi_x = \tan^{-1}\left(\frac{\omega_0(\tau_a-\tau_c-\tau_s)-\omega_0^3\tau_a\tau_c\tau_s}{1+\omega_0^2(\tau_a\tau_c+\tau_a\tau_s-\tau_c\tau_s)}\right)$$
$$\Phi_z = \omega_0\tau_s \tag{E.3}$$

Since dissipation is local and does not depend on the distance from the oscillating dipole, the phase difference is uniform throughout the medium and is an intrinsic function of the elastic parameters E and ν.

For two oscillating dipoles interacting through the strain field as outlined in the text (Eq. 4), and with the strains calculated from the Eq. E.2, one can assert that the result for the "local dissipation" model does not change the qualitative results for synchronization deduced for the "simple friction" model in the text. Consequently, for dipoles in close proximity as depicted in Fig. 2, the "in-phase" and "anti-phase" beating synchronization remains the same.

E.2 Network-fluid dissipation model

The Network-fluid model accounts for dissipation of energy that arises from the relative motion of water molecules with respect to the polymeric matrix. When the network is deformed by external forces (in this case cells modeled as force dipoles), the polymeric chains that comprise the gel network can move relative to the surrounding solvent molecules (water in hydrogels). This relative motion results in frictional shear forces that dissipate energy. For this "two-fluid model" [1], one can show that by coupling the equations of motion for the elastic medium to the Navier-Stokes equation for the solvent within the gel, the frictional force only affects the compressional mode, while the shear mode propagates infinitely fast [5]. This yields the expression for the frictional force shown in Table 1. However, the expression of Table 1 is only an approximation appropriate for long times $t > 4E(1-\nu)/\gamma(1+\nu)(1-2\nu)r^2$. Since we deal with dynamical steady-state, we must take extra care when decoupling the compressional and shear modes for dissipation. To this end, we correct the expression in Table 1 by adding a factitious, local friction term Γ that also affects the shear mode:

$$f_{fr} = -\frac{\gamma}{q^2}\frac{\partial}{\partial t}\nabla(\nabla\cdot\vec{u}) - \frac{\Gamma}{q^2}\frac{\partial}{\partial t}\vec{u} \tag{E.4}$$

Once a real space expression for $\vec{u}$ is obtained, we take the limit of $\Gamma \to 0$ to obtain the solution in the limit of fast propagation of shear mode. By doing so, we find that this corresponds to the limit of $\chi_s \to 0, \rho_s \to 0$ in Eq. A.8- A.11, yielding a simplified expression of the compressional mode alone. This does not qualitatively change the results for synchronization and indeed demonstrates how the "network-fluid" friction model is a simple version of the "simple-friction" model used throughout the text.

F One dimensional model for frequency matching

We model the beating cell as a 1-D viscoelastic system comprising a spring and dashpot connected in parallel, with a time dependent, active, contractile force $f_c(t)$ applied by the sarcomeres to the rest of the cell as well as an external, time dependent force $f_p(t)$ generated by the probe, and measured at the close vicinity of the cell (See Fig. F.1). The spring constant k_c is a measure of cellular elasticity which accounts in a coarse-grained manner for the elastic response of the cell to deformations of the cytoskelton. The "friction constant" γ_c is an outcome of both fluid-cytoskeleton friction in the cytosol as well as dissipation due to structural and activity differences in the sarcomeres that comprise the cell. The force balance equation due to a displacement δx from the equilibrium length is:

$$f_c(t) - \gamma_c \frac{d\delta x}{dt} - k_c \delta x + f_p(t) = 0 \tag{F.1}$$

We now suppose that the force exerted by the probe is a periodic function with frequency ω_p (single mode approximation). The force exerted by the cell is more generally treated as a sum of n different modes, each with frequency ω_j.

$$\begin{aligned} f_p(t) &= F_0 \cos \omega_p t \\ f_c(t) &= \textstyle\sum_{j=1}^{n} F_j \cos \omega_j t \end{aligned} \tag{F.2}$$

The power spectrum of the probe (with a single mode) and the cell are given by:

$$\begin{aligned} P_p &= \textstyle\int_0^\infty |f_p|^2 dt \; F_0^2 \\ P_c(n) &= \textstyle\int_0^\infty |f_c|^2 dt \sim \Sigma_{j=1}^{n} F_j^2 \end{aligned} \tag{F.3}$$

Using Fourier transform, the steady state displacement is calculated as:

$$\delta x(t) = \sum_{j=0}^{n} \frac{F_j}{(k_c^2 + \gamma_c^2 \omega_j^2)} \cos(\omega_j t + \phi_j) \quad \phi_j = \tan^{-1}(\frac{\gamma_c \omega_j}{k_c}) \tag{F.4}$$

One can see that the spring displacement is a superposition of the different modes in the system. The higher the frequency, the less that mode contributes to the sum, and the more out-of-phase it becomes.

Suppose that the cell has only one intrinsic frequency ω_c and an amplitude F_c that it is comparable with the frequency of the probe. Clearly, if the amplitude of the probe is far greater than the amplitude of the cell ($F_p \gg F_c$) the dominant contribution will come from the probe, and the entire system will oscillate with a frequency ω_p. Note that this is not synchronization, (since the cell does not adopt a new intrinsic frequency) but one frequency whose amplitude dominates the other.

However, if the cell can oscillate in n different modes, each with its own frequency ω_j and amplitude F_j, the comparison between the probe and cell oscillations is more subtle. A cell that can beat in many modes can be the result of

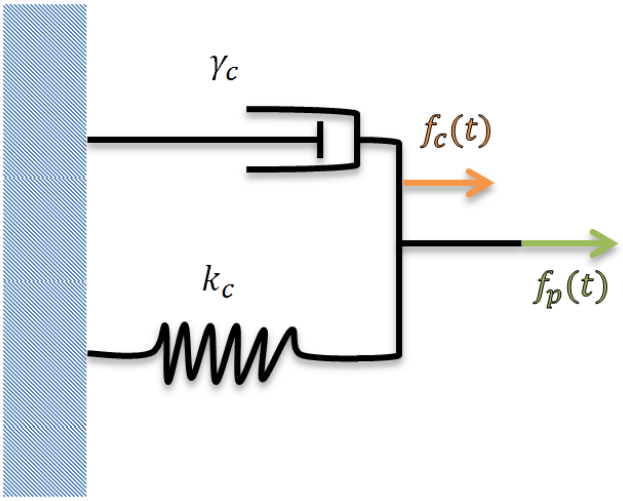

Figure F.1: A one dimensional model for a beating cardiomyocyte subjected to external probing. The viscoelastic nature of the cell is modeled as a spring and dashpot connected in parallel. The contractile force exerted by sarcomeric units within the cell is modeled by the periodic function $f_c(t)$, and the oscillating force applied by the probe is modeled by the periodic function $f_p(t)$.

the fact that the sarcomeres within the cell are not identical, and each beats with a different frequency and amplitude dictated by structural differences, availability of ATP etc. To compare this case to the one where the cell beats with a single frequency, we require that the power expended by the beating cell be the same, independent of the number of modes, n. This implies that the amplitude of each mode must be smaller than the amplitude of the single mode discussed previously ($F_j < F_c$). In that case, the probe can indeed dominate the beating amplitude of any one of the cell's intrinsic modes as soon as $F_p \gg F_{j,max}$. This is a much "softer" constraint compared with the previous case of single intrinsic frequency. Although complete synchronization (in terms of the Adler equation) is not possible in the absence of non-linearities, we see that cells that beat within a range of frequencies can be much more easily dominated by the probe deformation amplitude.

G Derivation of Adler equation

Jülicher and Prost [6, 7] have shown that active acto-myosin contractility combined with an elastic response (due in the case of sarcomeres to either the Z-body or actin deformations in response to contractility), result in an effective equation for the oscillator displacement as a function of time, x(t) that obeys the van der pol (VDP) equation for a non-linear oscillator:

$$\gamma\ddot{x} + r\dot{x} + \Lambda\dot{x}^3 + kx = f_{ext}(t) \tag{G.1}$$

While the van der Pol oscillator usually refers to the inertial response (represented by the "mass" γ) to a system which can have either positive ($r > 0$) or "negative friction" ($r < 0$) due to an input of energy, the standard inertia in low Reynolds number dynamics, is negligible. However, Jülicher and Prost show [6, 7] that acto-myosin dynamics results in an "effective mass" $\gamma > 0$ that is a function of the rate constants and binding energy. The unique characteristic of the VDP oscillator is that when the active input of energy dominates over the regular friction, so that $r < 0$, the system displays spontaneous oscillations at a frequency $\omega_c = \sqrt{k/\gamma}$ - even in the absence of an external driving force $f_{ext}(t)$. This is inherently different than a regular damped oscillator, where $r > 0$. To maintain stable oscillations, the non-linear term is essential, and $\Lambda > 0$ determines the amplitude of oscillations.

Introducing periodic forcing by an external probe/cell $f_{ext}(t) = F\cos(\omega_p t)$, which oscillates at a frequency that is, in general, different from the intrinsic frequency ω_c of the spontaneous oscillations, and rescaling all the coefficieets by the effective mass, γ, so that $\rho = r/\gamma$, $\lambda = \Lambda/\gamma$, $\alpha = F/\gamma$ we get:

$$\ddot{x} + \rho\dot{x} + \lambda\dot{x}^3 + \omega_c^2 x = \alpha\cos(\omega_p t) \tag{G.2}$$

We now find the criterion for the entrained regime, where the system oscillates at the probe frequency ω_p instead of its intrinsic frequency ω_c, where the solution has the form:

$$x(t) = a(t)e^{i\omega_p t} + a^*(t)e^{-i\omega_p t}, \quad a(t) = A(t)e^{i\Phi(t)}, \quad a^*(t) = A(t)e^{-i\Phi(t)} \tag{G.3}$$

where $A(t)$, $\Phi(t)$ are the time dependent amplitude and phase of oscillations respectively.

Since the process of synchronization is much slower than the characteristic frequency of the probe/cell (15 minutes compared to a time scale of 1 second, corresponding to ~ 1 Hz oscillations) we use the method of averaging – where we average over the slowest mode of oscillation [8]. Inserting Eq. G.3 into Eq. G.2, and averaging over the slowest mode (with a time scale given by $2\pi/\omega$) we write the dynamics of $a(t)$ as:

$$\begin{aligned}(\ddot{a} + 2i\omega_p\dot{a}) - (\omega_p^2 - \omega_0^2)a - \rho(\dot{a} + i\omega_p a) + \tfrac{\lambda}{4}\big(3\dot{a}^2(\dot{a^*} - i\omega_p a^*) \\ +6\dot{a}(aa^*\omega_p^2 + i\omega_p a\dot{a^*}) - 3a^2(\dot{a^*}\omega_p^2 - i\omega_p^3 a^*)\big) - \alpha = 0\end{aligned} \tag{G.4}$$

We now define the time scale $a/\dot{a} \sim \tau$ which is much longer than the time scale for oscillations $1/\omega_p$ (since the amplitude and phase are slowly varying). Because this time scale is long, for the terms that multiply λ and ρ separately, we consider only the lowest terms in $1/\tau$. For the same reasons, we neglect $\ddot{a}$ in the first term. Using the definitions in Eq. G.3 and comparing real and imaginary terms, we obtain two dynamical equations for the phase $\Phi(t)$and amplitude $A(t)$:

$$2\omega_p \dot{A} = \rho\omega_p A - \frac{3}{4}\lambda\omega_p^3 A^3 - \alpha\sin(\Phi) \tag{G.5}$$

$$2\omega_p A\dot{\Phi} = (\omega_0^2 - \omega_p^2)A - \alpha\cos(\Phi) \tag{G.6}$$

For weak forcing α, the dynamical equation for the amplitude becomes independent of phase, and one can calculate the steady-state amplitude $A_s = \sqrt{(4\rho/3\lambda\omega^2)}$. Introducing the steady state amplitude A_s into the dynamical equation for the phase, and making the further assumption that the frequency of forcing and the oscillator are relatively close (i.e. $\omega_c \sim \omega_p$) we obtain the Adler equation as presented in the text:

$$\dot{\Phi} = \omega_c - \omega_p - \frac{\alpha}{2\omega_p A_s}\cos(\Phi) \tag{G.7}$$

References

[1] DeGennes, P.G., Dynamics of entangled polymer solutions. i. the rouse model. *Macromolecules*, 1976, **9**, 587-593.

[2] Trappmann *et al.*, Extracellular matrix tethering regulates stem-cell fate. *Nature Materials*, 2012, **11**, 642-649.

[3] Landau, L. D. & Lifshitz, E. M., Course of Theoretical Physics, Theory of Elasticity *Pergamon Press Oxford*, 1986.

[4] Nitsan, I., Drori, S., Lewis, Y. E., Cohen, S. & Tzlil, S. Mechanical communication in cardiac cell synchronized beating. *Nature Phys.*, 2016, **12**, 472-477.

[5] Yuval, J. & Safran, S. A., Dynamics of elastic interactions in soft and biological matter. *Physical Review E*, 2013, **87**, 042703.

[6] Jülicher, F. Mechanical oscillations at the cellular scale. *Comptes Rendus de l'Académie des Sciences-Series IV-Physics-Astrophysics*, 2001, **2**, 849-860.

[7] Jülicher, F., Adjari, A. & Prost, J., Modeling molecular motors. *Rev. Mod. Phys.*, 1997, **69**, 1269-1281.

[8] Verhulst, F., Nonlinear differential equations and dynamical systems. Springer Science & Business Media, 2006.